International Journal of Pharmaceutics 391 (2010) 248–259

Contents lists available at ScienceDirect

International Journal of Pharmaceutics

journal homepage: www.elsevier.com/locate/ijpharm

Pharmaceutical Nanotechnology

Biophysical characterization of a liposomal formulation of cytarabine and daunorubicin

Awa Dicko, Sungjong Kwak, April A. Frazier, Lawrence D. Mayer, Barry D. Liboiron*

Celator Pharmaceuticals Corp., 1779 W 75th Avenue, Vancouver, BC, V6P 6P2 Canada

ARTICLE INFO

Article history:
Received 26 November 2009
Received in revised form 26 January 2010
Accepted 8 February 2010
Available online 13 February 2010

Keywords:
Cytarabine
Daunorubicin
Liposomes
Copper gluconate
EPR
CPX-351

ABSTRACT

The biophysical characterization of CPX-351, a liposomal formulation of cytarabine and daunorubicin encapsulated in a synergistic 5:1 molar ratio (respectively), is presented. CPX-351 is a promising drug candidate currently in two concurrent Phase 2 trials for treatment of acute myeloid leukemia. Its therapeutic activity is dependent on maintenance of the synergistic 5:1 drug:drug ratio in vivo. CPX-351 liposomes have a mean diameter of 107 nm, a single phase transition temperature of 55.3 °C, entrapped volume of 1.5 μL/μmol lipid and a zeta potential of −33 mV. Characterization of these physicochemical properties led to identification of an internal structure within the liposomes, later shown to be produced during the cytarabine loading procedure. Fluorescence labeling studies are presented that definitively show that the structure is composed of lipid and represents a second lamella. Extensive spectroscopic studies of the drug–excipient interactions within the liposome and in solution reveal that interactions of both cytarabine and daunorubicin with the copper(II) gluconate/triethanolamine-based buffer system play a role in maintenance of the 5:1 cytarabine:daunorubicin ratio within the formulation. These studies demonstrate the importance of extensive biophysical study of liposomal drug products to elucidate the key physicochemical properties that may impact their in vivo performance.

1. Introduction

Liposomes have been investigated widely as parenteral drug delivery vehicles. They have been applied most extensively to the delivery of antineoplastic agents where an improved therapeutic index for numerous drugs has been shown to be mediated by a decrease in drug toxicity and/or an increase in therapeutic potency (Boman et al., 1994; Park, 2002). Historically, efforts have focused on formulating individual anticancer drugs, however due to the prevalent use of combination chemotherapy to treat most types of cancer; increasing attention has been given to delivering drug combinations (Sengupta et al., 2005; Mayer et al., 2006).

Work in our laboratory and others has demonstrated that whether drug combinations interact synergistically, additively or antagonistically can depend on the ratio of the drugs exposed to cancer cells (Mayer et al., 2006; Harasym et al., 2007a). Consequently, the retention of drug combinations encapsulated and delivered in liposomes must be coordinated in order to avoid the deleterious effects of exposing antagonistic drug ratios to cancer cells in vivo. We have demonstrated that designing liposomes which maintain synergistic drug ratios after administration in vivo markedly improved the efficacy of several drug combinations over their free drug cocktail counterparts (Mayer et al., 2006; Mayer and Janoff, 2007; Harasym et al., 2007a,b; Tardi et al., 2007, 2009a,b). These results have provided the scientific basis for advancing such synergistic fixed-ratio liposome formulations into clinical testing (Batist et al., 2007, 2009).

CPX-351 is a liposomal formulation of cytarabine and daunorubicin co-encapsulated and delivered at a 5:1 molar ratio shown to be synergistic both in vitro and in vivo (Bayne et al., 2009; Tardi et al., 2009b). Preclinical studies revealed that CPX-351 dramatically increased the therapeutic activity compared to the unencapsulated cytarabine plus daunorubicin combination, which is standard of care treatment for acute myeloid leukemia (AML), in a wide range of leukemia tumor models (Tardi et al., 2009b) Furthermore, CPX-351 has displayed promising signs of antileukemic activity in a Phase I trial with relapsed and refractory acute leukemia patients and is currently being evaluated in two randomized Phase II clinical trials in patients with newly diagnosed AML and first relapse AML.

CPX-351 has been shown to maintain the 5:1 molar ratio of cytarabine:daunorubicin for more than 24 h after intravenous (IV) administration both preclinically and clinically (Tardi et al., 2009b). Such coordinated pharmacokinetics was achieved by manipulations in the liposome membrane composition as well as excipient–drug interactions (Dicko et al., 2007; Tardi et al., 2007). In addition to the structural characteristics of the lipo-

* Corresponding author. Tel.: +1 604 708 5858; fax: +1 604 708 5883.
E-mail address: bliboiron@celatorpharma.com (B.D. Liboiron).

0378-5173/$ – see front matter © 2010 Elsevier B.V. All rights reserved.
doi:10.1016/j.ijpharm.2010.02.014

some membrane, the physicochemical interactions between drugs and excipients likely modulate the drug disposition and retention inside liposomes. The latter feature is particularly germane since the intraliposomal space of CPX-351 liposomes contains copper gluconate, triethanolamine (TEA), cytarabine and daunorubicin. In the present study, detailed biophysical studies were undertaken to characterize basic physicochemical properties of CPX-351 as well as to delineate specific drug–excipient interactions associated with the coordinated retention of the two drugs.

2. Materials and methods

2.1. Materials

Distearoylphosphatidylglycerol (DSPG), distearoylphosphatidylcholine (DSPC) and cholesterol (Chol) were obtained from Avanti Polar Lipids (Alabaster, AL, USA). Cytarabine ($pK_a = 4.2$, $\log P = -2.15$ (Product Monograph, Pfizer Canada, 2008) and daunorubicin ($pK_a = (13.6), 9.9, 8.49$ (May et al., 1985); $\log P$ (ACD $\log P$) = 2.9, $\log D$ (ACD $\log P$) = 1.23 (pH 7.4)) were obtained from Drug Source Company (Westchester, IL, USA). Copper gluconate was purchased from Purac (Lincolnshire, IL, USA). All other chemicals were obtained from Sigma Chemical Company (St. Louis, MO, USA).

2.2. Preparation of the formulations

The liposomes were generated by a solvent emulsion and size reduction procedure as previously described (Tardi et al., 2009a). Briefly, the lipids (DSPC/DSPG/Chol: 7/2/1, mol%) were dispersed in neutral pH solutions of 50 mM copper gluconate, 110 mM TEA; 10 mM copper gluconate, 22 mM TEA (referred to as low copper formulation) or 100 mM sodium gluconate, 110 mM TEA (referred to as copper-free formulation). The liposomes were extruded at 70 °C through 100 nm polycarbonate filters using an extruder apparatus (Northern Lipids, Vancouver, BC) until the mean diameter of the formulations were 100 ± 20 nm as determined by dynamic light scattering.

The encapsulation of cytarabine was carried out by mixing solutions of cytarabine and liposomes in the above buffers and incubating the resultant mixture beyond the phase transition temperature (55 °C) until a drug:lipid ratio of 0.5 was achieved (overall encapsulation efficiency = 5%). To determine encapsulated cytarabine, 100 μL aliquots of the loading mixture were removed at appropriate timepoints and applied to a Sephadex G-50 spin column to remove the unencapsulated cytarabine. The columns were prepared by adding glass wool to a 1 mL syringe and Sephadex G-50 beads hydrated in sucrose phosphate buffer (SUP) at neutral pH. The columns were packed by spinning at 290 g for 1 min. Following addition of the sample to the column, the liposome fraction was collected in the void volume by centrifuging at 515 g for 1 min. The drug:lipid ratio at each time point was obtained by determining the concentration of cytarabine and lipids in the spin column eluents using high performance liquid chromatography (HPLC).

For liposomal formulations containing daunorubicin, the drug was dissolved in sucrose phosphate ethylenediaminetetraacetic acid (EDTA) buffer (SPE) at neutral pH, warmed and incubated with the cytarabine-loaded liposomes for 10 min to achieve the desired daunorubicin:lipid (0.1:1 mol/mol, ~100% encapsulation efficiency) or daunorubicin:cytarabine (1:5 mol/mol) ratio. The unencapsulated drug was removed by exchanging the external liposomal buffer into sucrose phosphate buffer at neutral pH using tangential flow chromatography. The concentration of daunorubicin in the liposomes was determined by HPLC. Daunorubicin leakage from copper-free liposomes was evaluated by visual observation of the orange colour in the eluent during dialysis at room temperature.

2.3. Differential scanning calorimetry (DSC)

Data were collected on a PerkinElmer Pyris 1 Calorimeter (PerkinElmer Life and Analytical Sciences, Woodbridge, ON) calibrated using an Indium standard with an onset temperature of 156.6 ± 0.5 °C. The CPX-351 formulation was thawed at ambient temperature for 1 h. A 20 μL aliquot was loaded into a 50 μL metal pan (PerkinElmer, ON) and placed into the sample holder. An empty metal pan was used as reference. The thermogram was recorded from 25 °C to 70 °C at a scanning rate of 1 °C/min. At the end of the run, a baseline correction of the thermogram was performed and the main gel to liquid–crystalline phase transition temperature was determined.

2.4. Zeta potential

Measurements were made using a ZetaPALS zeta potential analyzer (Brookhaven Instruments, Holtsville, NY) calibrated using the NIST SRM1980 electrophoretic mobility standard. The electrodes were soaked in a 1 cm cuvette containing a solution of CPX-351 at 1 mg/mL lipid in sucrose phosphate buffer. Each analysis was made using three 60-cycle runs. Each sample was analyzed in triplicate. The average zeta potential and the standard deviation of the three analyses were reported.

2.5. Trapped volume

The trapped volume was determined using CPX-351 enriched with ^3H-H_2O and ^{14}C-lactose as described by Perkins et al. (1993). This method is based on the fact that water is freely permeable across lipid membranes whereas lactose does not pass through lipid bilayer membranes in the absence of significant external perturbation and is thereby excluded from the volume occupied by the liposomes. The radiolabeled solutions were added to the thawed CPX-351 formulation. The sample was briefly vortexed and allowed to equilibrate for 10 min at ambient temperature. Samples were centrifuged using Microcon YM-30 centrifugal filter units at 15,700 × *g* for 1 h and counted for radioactivity on a Beckman Coulter LS 6500 Liquid Scintillation Counter (Beckman Coulter Canada, Mississauga, ON). Comparison of the ratio ^3H-H_2O/^{14}C-lactose before and after centrifugations allowed determination of the amount of ^{14}C-lactose that was excluded from the liposomes as reflected by the enrichment of ^{14}C-lactose counts relative to the ^3H-H_2O counts. The amount of excluded ^{14}C-lactose was compared to the known lipid concentration (converted to μmol/mL) and the trapped volume was calculated.

2.6. Cryogenic transmission electron microscopy

The cryogenic transmission electron microscopy (cryo-EM) investigations were performed with a Zeiss EM 902A Transmission Electron Microscope (Carl Zeiss NTS, Oberkochen, Germany). The procedure used for sample preparation and image recording is described in Almgren et al. (2000). Briefly, a small drop (~1 μL) of sample was deposited on a copper grid covered with a perforated polymer film covered with a thin carbon layer on both sides. Excess liquid was removed by means of blotting with a filter paper, leaving a thin film of the solution on the grid. Immediately after blotting, the sample was vitrified in liquid ethane, held just above its freezing point. Samples were kept below −165 °C and protected against atmospheric conditions during both transfer to the microscope and

examination. Images were recorded under low dose conditions at 105,000× magnification with a defocus of 3 μm.

2.7. Electron paramagnetic resonance (EPR) spectroscopy

X-band EPR spectra were acquired in a liquid nitrogen finger dewar at 77 K, using a Bruker ESP300E continuous wave spectrometer. Typical acquisition parameters were: sweep width 2300–3900 G, modulation amplitude 10 G at 100 kHz, microwave power 10 mW at 9.45 GHz. A Hewlett-Packard Model 5253B microwave frequency counter and Bruker ER035 NMR Gaussmeter were used to calibrate the microwave and magnetic fields, respectively. Baseline correction and double integration for spin quantification of acquired spectra were carried out using Bruker WinEPR software (v. 2.11b). The intensities of the doubly integrated spectra were compared against the intensity of a known copper standard (1.0 mM $CuCl_2$ in 0.01 M HCl with 2 M $NaClO_4$) (Carithers and Palmer, 1981), acquired under identical conditions, to obtain the molar concentration of paramagnetic species present in the sample. Simulation of experimental spectra was completed with Bruker SimFonia software (v. 1.26β). Samples were measured in 714-PQ 4 mm clear fused quartz tubes from Wilmad/LabGlass (Buena, NJ).

2.8. ^1H nuclear magnetic resonance (NMR) spectroscopy

Proton NMR spectra were recorded on a Bruker (Oakville, ON) Avance 400 MHz spectrometer equipped with a 5 mm direct broadband probe. Spectra were recorded in 5 mm Norell (Landisville, NJ) type 507 NMR tubes at room temperature using the "zgpr" pulse pattern for water peak suppression. NMR spectra were processed using ACDLabs v. 10.0.0 ACD/SpecManager (Advanced Chemistry Development, Toronto, ON).

2.9. Osmolality measurements

The osmolality of 50 mM copper gluconate, 110 mM TEA, pH 7.4 in the absence and presence of cytarabine was measured using a micro-osmometer (Model 3320, Advanced Instruments Inc.) calibrated with two commercial standards (Advanced Instruments Inc.).

2.10. Dynamic light scattering (DLS)

Dynamic light scattering for measurement of liposome size distribution was carried out on a NICOMP Model 370 (Particle Sizing Systems Inc., Santa Barbara, CA). Liposome samples were typically diluted to ~1 mg/mL total lipid in saline or SPE buffer, placed in 6 mm × 50 mm glass culture tubes (Kimble–Kontes, Vineland, NJ) and measured for 10 min. Differences in buffer viscosity and refractive index were accounted for in the fitting of the autocorrelation function.

2.11. Ultraviolet–visible (UV–vis) electronic absorption spectroscopy

UV–vis spectra were acquired using a Shimadzu scanning UV-2401 spectrophotometer (Shimadzu Scientific Instruments, Columbia, MD), equipped with a Shimadzu Peltier device, for temperature control. Spectra were acquired at 25 °C, fast scan speed with 1 nm data pitch and 1 nm slits, in 1 cm or 0.01 cm cuvettes as appropriate.

2.12. Fluorescence spectroscopy

A small batch of 7:2:1 unilamellar DSPC/DSPG/Chol (7/2/1 mol%) liposomes containing low levels of a fluorescent probe lipid (*N*-(7-nitrobenz-2-oxa-1,3-diazol-4-yl)-1,2-dihexadecanoyl-*sn*-glycero-3-phosphoethanolamine, NBD-PE, ~0.01 mol%, Invitrogen, Carlsbad, CA) was made. A portion of the labeled liposomes was subsequently loaded with cytarabine in a manner analogous to the procedure used for CPX-351. Two samples were prepared for fluorescence analysis: unloaded and cytarabine-loaded liposomes. Each sample was buffer exchanged by tangential flow into SPE buffer and sized by DLS in saline solution.

Each sample was diluted in SPE buffer to ~2 mM lipid and the fluorescence emission spectrum (λ_{ex} = 450 nm) was measured between 480 nm and 600 nm using a Cary Eclipse fluorescence spectrophotometer (Varian, Palo Alto, CA). To study the relative amounts of NBD label exposed to the external buffer, a small amount of sodium dithionite (~50 mg) was added to the sample, the suspension vortexed briefly, and the fluorescence emission spectrum was re-measured periodically over a total period of 75 min.

3. Results

The focus of these studies was to evaluate CPX-351 for a range of core physical features that are relevant to virtually all liposome products as well as to establish product-specific parameters based on a variety of spectroscopic and biochemical techniques. These data can be used to identify relationships between specific physicochemical properties and functional performance as well as help to establish key physicochemical tests that can serve as quality indicators. The physicochemical investigations described here were conducted in order to expand our understanding of the physical disposition of the components contained in CPX-351.

3.1. Core physicochemical properties

We refer to core physicochemical properties as those basic features that will be present in virtually all liposome-based pharmaceutical drug products. These properties include phase transition temperature, liposome morphology, lamellarity, volume of entrapment inside the liposomes and surface charge.

Differential scanning calorimetry was utilized to monitor the melting phase transition of the liposomes in CPX-351. The bilayer membrane of CPX-351 liposomes is composed of DSPC, DSPG and cholesterol at a molar ratio of 7:2:1. DSPC and DSPG are saturated, long chain phospholipids with melting transition temperatures of 55.5 °C and 54.5 °C, respectively (Cevc, 1993). Although cholesterol is able to abolish the melting transition of saturated phospholipids, elevated membrane concentrations (≥30 mol%) are required to achieve this effect (McElhaney, 1982) and consequently, the liposomes of CPX-351 undergo a gel to liquid–crystalline phase transition in a temperature range corresponding to the melting temperatures of the individual phospholipids (Table 1).

Table 1
Core physicochemical parameters of drug-free liposomes and CPX-351.

	Size (nm)[a]	Polydispersity[a]	T_m (°C, σ^2 = 0.5)	Zeta Potential (mV, σ^2 = 5)	Trapped volume (μL/μmol lipid) (σ^2 = 0.3)
Drug-free liposomes	114.8[b] (8)	0.25 (1)	55.5	−32	1.6
CPX-351	107.2[b] (1)	0.243 (5)	55.3	−33	1.4

[a] Number in parentheses represents the standard error of the mean in the last reported digit. Six (drug-free) or three (CPX-351) measurements were made.
[b] Significant difference, $\alpha < 0.05$.

The surface charge of CPX-351 was assessed by performing zeta potential measurement. Since the lipid membrane in CPX-351 contains 20 mol% DSPG, a negatively charged phospholipid, these liposomes should exhibit a negative surface potential and hence, a negative zeta potential. The loss of a strong negative zeta potential for the liposomes in CPX-351 would be indicative of significant surface changes that could lead to altered drug retention and plasma elimination properties after in vivo administration. As shown in Table 1, CPX-351 has a negative surface potential of −33 mV that is expected to provide strong Coulombic repulsive forces that would overcome van der Waals attractions, thereby imparting increased particle stability. Furthermore, the zeta potential value of CPX-351 was similar to that of the drug-free liposomes (−32 mV) suggesting that the presence of both drugs did not alter the lipid membrane stability.

The entrapped aqueous volume of liposomes impacts the amount of drug that can be encapsulated per micromole of liposomal lipid. Generally, increasing liposome size increases the trapped volume. The trapped volume of CPX-351 is determined by spiking samples with ^{3}H-H_2O and ^{14}C-lactose, as described in Section 2. The mean aqueous trapped volume of CPX-351 liposomes is 1.4 μL/μmol lipid (Table 1). This value is slightly less than that of the unloaded liposomes (1.6 μL/μmol lipid).

We used cryogenic transmission electron microscopy to visualize the lipid vesicles in CPX-351. Fig. 1A shows that the liposomes of CPX-351 present faceted surface morphology caused by the growth of gel-phase lipid planes upon cooling below the lipid melting phase transition temperature. In addition, a spherical internal structure is consistently observed within the CPX-351 liposomes. Since the drug-free liposomes did not show this inner feature (Fig. 1B), it was first postulated that this structure corresponds to daunorubicin–copper gluconate/TEA precipitate. This was supported by previous studies where the formation of internal structures was attributed to doxorubicin precipitate inside liposomes containing either citrate buffer (Cullis et al., 1997; Li et al., 1998) or ammonium sulfate (Lasic et al., 1992, 1995; Haran et al., 1993; Abraham et al., 2002).

Since the production of CPX-351 is a two-step drug loading process, we performed cryo-EM on the cytarabine-loaded liposomes before the addition of daunorubicin. Interestingly, the internal structure was also present in cytarabine containing liposomes (Fig. 1C), thus ruling out the first hypothesis of a daunorubicin precipitate. Previous studies have shown that copper can form complexes with nucleosides and nucleotides (Berger and Eichhorn, 1971; Chao and Kearns, 1977). Under our experimental conditions, it is possible that at high intraliposomal concentrations, cytarabine forms an insoluble complex with copper gluconate that could be responsible for the observed internal structure. Another hypothesis was to attribute the inner feature to a second lipid bilayer formed upon membrane invagination, due to transbilayer surface area imbalances (Mui et al., 1995; Cullis et al., 1997). In order to unequivocally prove the nature of this ring, we undertook a series of experiments using fluorescence spectroscopy.

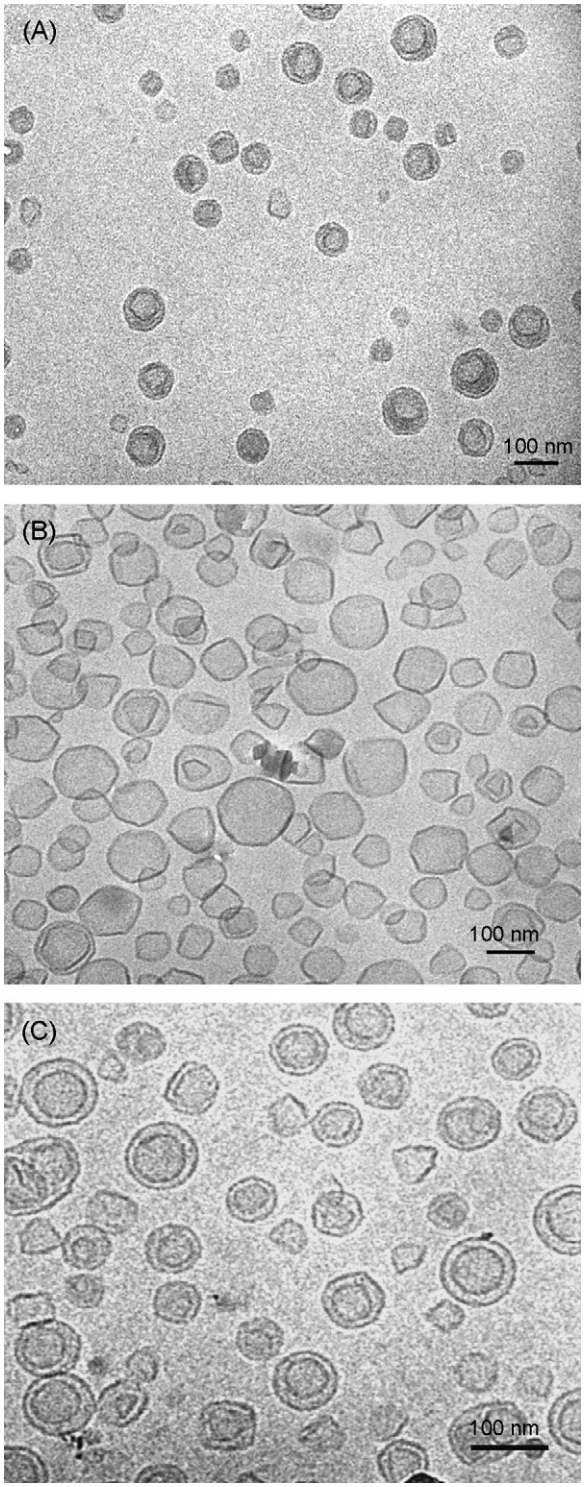

Fig. 1. Cryo-EM images of (A) CPX-351; (B) post-extrusion liposomes and (C) liposomes after cytarabine loading. The scale bar represents 100 nm.

3.2. Composition of the internal structure of CPX-351

Fluorescence quenching of NBD-PE-labeled liposomes was performed to verify the hypothesis that the internal structure in CPX-351 liposomes was in fact an additional lipid vesicle. This lipid probe (Fig. 2A), structurally similar to phospholipids, possesses a head group label of the strongly fluorescent 7-nitrobenzofurazan and has the distinct advantage that it can be irreversibly quenched through chemical reduction of the nitro group (Fig. 2B). Liposomes have been shown to be impermeable to sodium dithionite at ambient temperature and thus only those NBD moieties exposed to the external buffer will be reduced (McIntyre and Sleight, 1991; Angeletti and Nichols, 1998). NBD-PE molecules associated with the inner leaflet or an internal lipid structure would be protected from reduction and therefore continue to emit fluorescence in the presence of dithionite. This concept is presented in a schematic diagram in Fig. 2C.

The spectra of unilamellar and bilamellar liposomes are shown in Fig. 3A and B, respectively. The time course of the fluorescence intensity at 528 nm is shown in Fig. 3C. As the reduction reaction proceeded, the fluorescence intensity of both samples

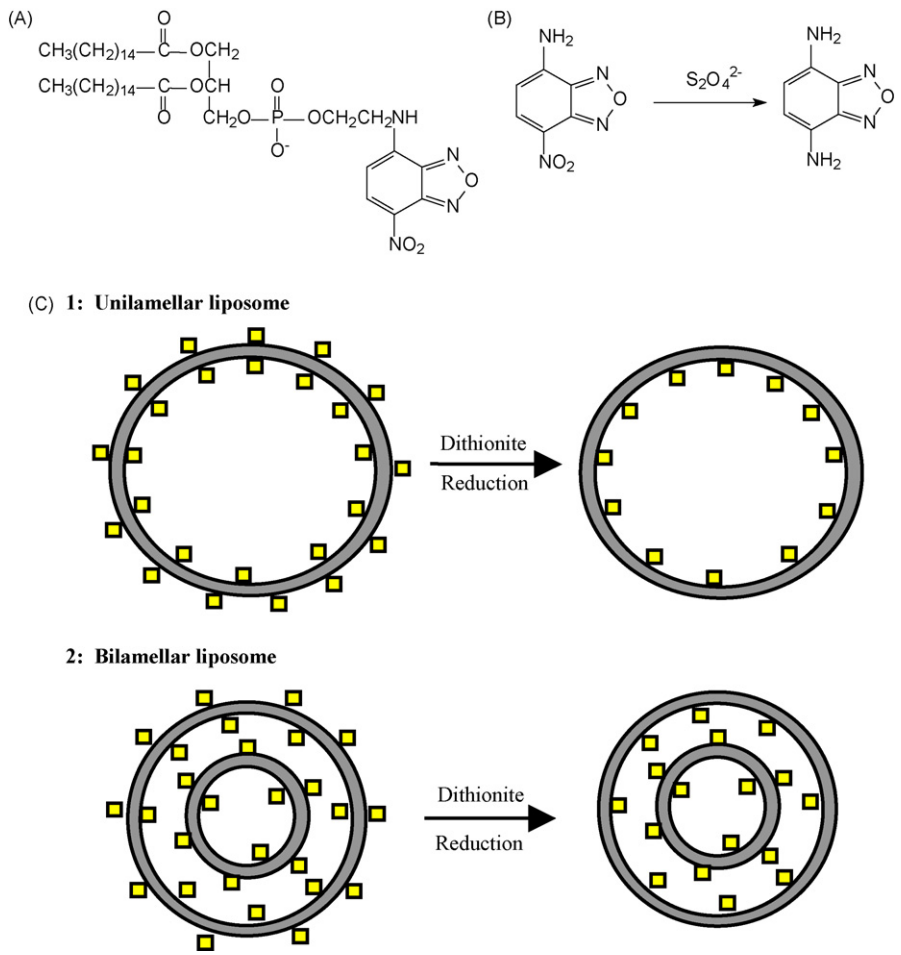

Fig. 2. (A) Structure of *N*-(7-nitrobenz-2-oxa-1,3-diazol-4-yl)-1,2-dihexadecanoyl-*sn*-glycero-3-phosphoethanolamine (NBD-PE). (B) Chemical reduction of NBD (left) by dithionite, $S_2O_4^{2-}$, completely quenches the fluorescence emission of NBD. (C) Representation of differences in solvent accessibility of NBD-labeled lipid (represented as squares) for (1) unilamellar and (2) bilamellar liposome systems. Dithionite, a membrane impermeant reductant, irreversibly reduces all NBD-labeled lipids exposed to the external buffer. This reduction completely quenches NBD fluorescence. In a bilamellar system, a greater proportion of the total lipid is protected from reduction inside the liposome, the ratio of which is dependent on the radius of the inner vesicle.

decreased, however the residual fluorescence intensity remaining in the two samples, normalized to the initial intensity prior to the addition of sodium dithionite, varied by approximately 15%. The unloaded sample was quenched by 54% (46% unquenched) and the cytarabine-loaded sample experienced a 39% drop in fluorescence intensity at 528 nm (61% unquenched). This result indicates that a greater portion of the total lipid is protected from chemical reduction in the cytarabine-loaded system, despite the similar average liposomal diameter. More insights into the physicochemical disposition of drugs and excipients were determined through extensive characterization of CPX-351 using EPR and NMR spectroscopy.

3.3. Spectroscopic features of CPX-351

The physical and chemical states of encapsulated drugs within liposomes have been shown to strongly affect their pharmacokinetic properties (Dicko et al., 2008). We therefore undertook a detailed spectroscopic study of CPX-351 and its components in solution to describe the intraliposomal drug–excipient interactions.

The presence of the paramagnetic copper(II) ion in the copper gluconate/TEA buffer system used in CPX-351 allowed application of electron paramagnetic resonance spectroscopy to investigate the intraliposomal coordination state of the buffer. EPR is a sensitive, selective spectroscopic technique based on magnetic resonance signals akin to NMR that arise from unpaired electron(s) in an external magnetic field. Signal intensity is directly proportional to the concentration of paramagnetic species through the use of a spin standard and double integration of the acquired spectrum.

Fig. 4 shows a typical EPR spectrum at 77 K of CPX-351. Two main features are evident. The first is the appearance of two clear lines in the parallel region at 2720 G and 2900 G, with suggestion of a third at 3080 G. This analysis yields a crude estimate of a ~180 G hyperfine splitting, which is due to a single paramagnetic copper center. Simulation of the parallel region of the spectrum yields $g_{||} = 2.265$ and $A_{||} = 184 \times 10^{-4}$ cm^{-1}. The fourth predicted hyperfine line would appear at ~3250 G, buried underneath the strong perpendicular peak. The second feature is the very broad perpendicular peak centered at 3300 G, nearly double the linewidth typically observed for isolated, magnetically dilute copper(II) centers. To assign these spectroscopic features observed within CPX-351 liposomes, we conducted spectroscopic studies of relevant species in solution, presented below.

3.3.1. Interaction of cytarabine and copper gluconate/TEA in solution by EPR

Interaction of cytarabine with copper gluconate/TEA buffer at pH 7.4 was monitored in solution by EPR. A set of samples were prepared to which was added varying amounts of cytarabine. The samples were frozen and the EPR spectra measured at 77 K (Fig. 5), with the resultant spectra doubly integrated to yield the concentration of observable copper(II). The spin integration results reported

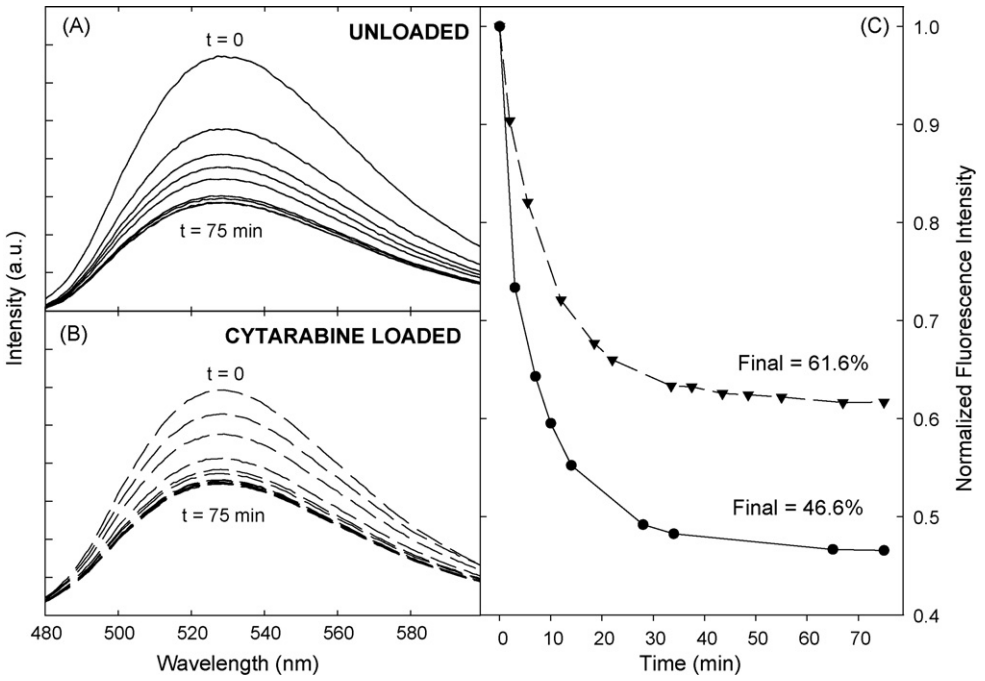

Fig. 3. Quenching of NBD-PE fluorescence of NBD-PE labeled (~0.01%) liposomes (SPE buffer, pH 7.4) over time by sodium dithionite (λ_{ex} = 450 nm). (A) Unloaded liposomes. (B) Cytarabine-loaded liposomes. (C) Reduction in fluorescence emission intensity at 528 nm for unloaded (solid line, ●) and cytarabine-loaded (dashed line, ▼) liposomes labeled with NBD-PE (~0.01%), exposed to excess sodium dithionite in the external buffer.

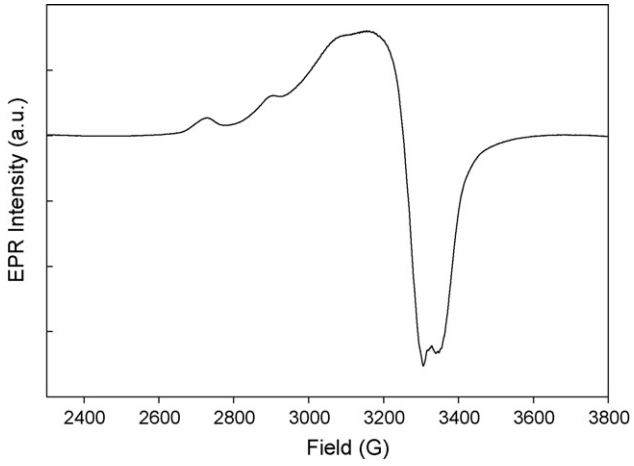

Fig. 4. EPR spectra of CPX-351 (T = 77 K, P = 10 mW, modulation amplitude = 10 G, ν = 9.45 GHz, 9 scans).

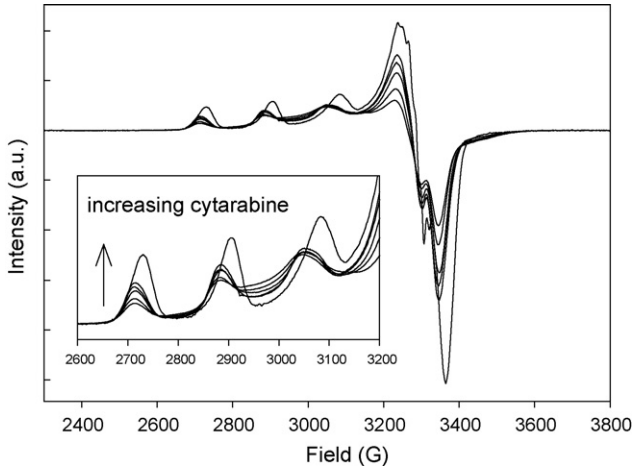

Fig. 5. EPR spectra of copper gluconate/TEA (pH 7.4) titrated with cytarabine, normalized to total copper concentration. Inset: magnification of the parallel region of the EPR spectrum. Spectra are plotted from the bottom up, from the least intense to most intense: [Cu] = 2.5 mM (normalized), [cytarabine] = 0 mM, 5 mM, 19 mM, 23 mM, 29 mM and 930 mM.

in Table 2 reveal that a 1:2 solution of copper(II) and sodium gluconate at pH 7.4 is comprised largely of a highly stable copper dimer ($\log\beta$ = 18.9) with an empirical formula of $[Cu_2(Glu)_2OH]^-$, in agreement with earlier thermodynamic potentiometry studies (Pecsok and Juvet, 1955; Escandar and Sala, 1992). This complex

Table 2
Total paramagnetic copper observed by EPR for copper gluconate/TEA titration by cytarabine, as monitored by double integration of the EPR spectrum.

[CuGlu], mM	[TEA], mM	[cytarabine], mM	Spin intensity[a] (×10^4)	Observable [Cu], mM	% Observable Cu
4.0	0	0	0.45	0.14	3.6
17.5	38.5	0	6.80	2.17	12.4
17.5	38.5	26	6.93	2.21	12.6
17.5	38.5	66	7.63	2.43	13.9
17.5	38.5	106	7.89	2.51	14.4
17.5	38.5	130	8.37	2.67	15.2
2.5	5.5	930	1.65	0.52	21.0

[a] Total spin number from double integration, normalized to number of scans and instrument gain.

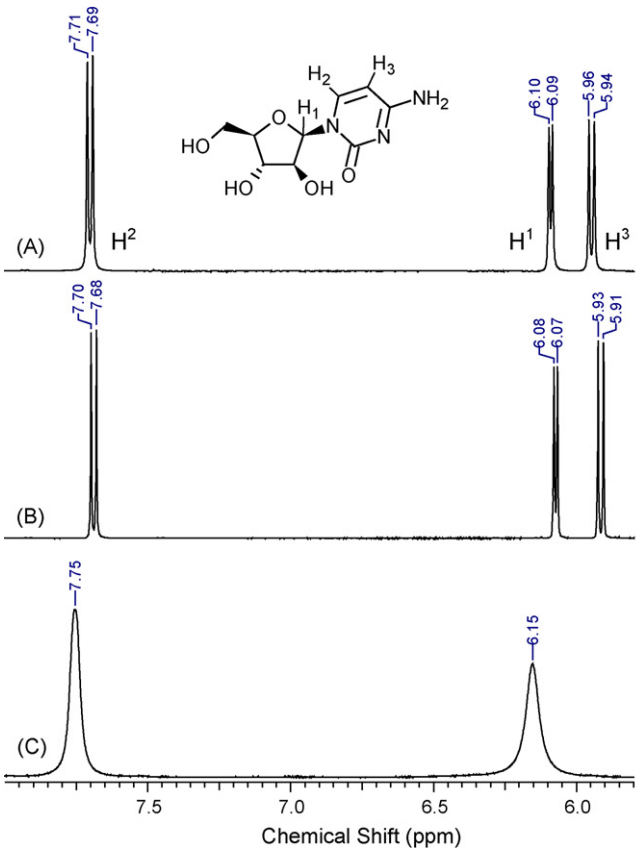

Fig. 6. Aromatic region of the 400 MHz ^{1}H NMR spectra of (A) 50 mM cytarabine in D_2O; (B) 100 mM cytarabine in 100 mM sodium gluconate, 110 mM TEA, pH 7.4; (C) 100 mM cytarabine in 50 mM copper gluconate/TEA, pH 7.4. Inset: chemical structure of cytarabine with the three observable protons of this spectral region assigned.

is mainly EPR-silent, presumably due to antiferromagnetic coupling between the copper centers. Addition of 2 equiv. of TEA to this solution increases the EPR-observable fraction of a 1:2 solution of copper(II) and gluconic acid at pH 7.4 from 3% to 12% (Table 2) most likely by breaking some of the dominant dimer to make monomeric copper complexes that are EPR-active. Further addition of cytarabine into the study solution increases the signal intensity from the initial value of 12% for copper gluconate with 2 Mequiv. of TEA, up to 22% observable copper for CuGluTEA with a large (340 Mequiv.) excess of cytarabine.

3.3.2. Interaction of cytarabine and copper gluconate/TEA in solution by ^{1}H NMR

The observation that cytarabine interacts with the copper gluconate/TEA buffer at pH 7.4 was confirmed by ^{1}H NMR spectroscopy (Fig. 6). The aromatic proton region of the NMR spectrum of a solution of cytarabine in deuterated phosphate buffer at pD 7.4 (Fig. 6A) was measured and compared to the spectrum of cytarabine (100 mM) in 100 mM sodium gluconate, 110 mM TEA, pH 7.4 (Fig. 6B), and 50 mM copper gluconate, 110 mM TEA buffer at pH 7.4 (Fig. 6C). The cytarabine NMR spectrum was similar to the spectrum available in the ACD/Labs spectral database and assigned based on that analysis. For the spectrum acquired in 50 mM copper gluconate/TEA buffer (pH 7.4) (Fig. 6C), a clear broadening of all peaks is observed, in addition to the complete absence of one resonance observed at $\delta \sim 5.95$ in the copper-free spectra A and B. The presence of sodium gluconate and/or TEA does not affect the observation of this peak (Fig. 6B), demonstrating that the loss of this peak in Fig. 6C is due to the presence of copper. The proton that corresponds to this resonance (labeled as H_3 in the inset chemical structure of cytarabine) is assigned as the aromatic proton *ortho* to the primary amine and *meta* to the ring imine nitrogen, which together comprise the most likely site for Cu(II) coordination. Direct coordination to the drug would be expected to completely obscure adjacent protons due to excessive broadening. The other ring proton, *para* to the imine nitrogen (labeled H_2 in the inset structure), does appear in the spectrum, but like all other peaks is considerably broadened. Therefore, EPR and NMR solution studies of copper gluconate/TEA interactions with cytarabine confirm a weak, transient interaction of the drug with the buffer system at the drug:metal ratio found within CPX-351 (2:1 cytarabine over copper).

3.3.3. Stoichiometry of daunorubicin–copper complex by UV–vis

During daunorubicin encapsulation, the colour of the liposome solution changes from a deep red-orange to purple due to a shift in the absorbance maximum from 480 nm to 545 nm (Fig. 7A). This colour change indicates that daunorubicin is interacting with some species inside the liposomes. The stoichiometry of the reaction leading to the observed changes in the UV–vis absorbance spectrum of daunorubicin during drug loading was studied via a batch titration. Daunorubicin was titrated with copper gluconate/TEA (1:0.2 mol/mol), pH adjusted to 7.4 with NaOH. The resulting UV–vis spectra are shown in Fig. 7B. As the relative concentration of copper to daunorubicin increases, the peak maximum shifts from 480 nm to 545 nm. This change is accompanied by a general loss of spectral intensity. These spectral changes are monitored by plotting the ratio of 480 nm to 545 nm absorbance as a function of copper:daunorubicin ratio (Fig. 7C). Addition of small amounts of copper gluconate to the daunorubicin solution lead to large changes in the 480:545 nm absorbance ratio, from an initial value for free daunorubicin of ~2.5 to a final value of ~0.7 after addition of 2 Mequiv. of copper (as copper gluconate/TEA). Of note in Fig. 7 is the change in 480:545 nm absorbance ratio; after addition of ~1.0 equiv. of copper, there is little further spectral change. This suggests the dominant stoichiometry for complex formation is one daunorubicin ligand to one Cu(II) center.

3.3.4. Interaction of daunorubicin and copper gluconate/TEA by EPR

The obvious colour change upon daunorubicin encapsulation in CPX-351 led to the investigation of copper buffer interactions with daunorubicin by EPR. As with the studies conducted with cytarabine, EPR spectra of copper gluconate/TEA buffer with varying amounts of daunorubicin were acquired to gain insights into the interaction stoichiometry and the effect of daunorubicin on the coordination state of the copper gluconate/TEA system.

Fig. 8 depicts the EPR spectra of a 1:1 and 1:5 copper gluconate/TEA:daunorubicin solution. These spectra are markedly different from those presented in the previous section for copper gluconate/TEA and cytarabine. In the 1:1 copper gluconate/TEA:daunorubicin spectrum, the perpendicular region between 2900 G and 3500 G is very broad and derivative-shaped. An additional negative signal is found at ~3550 G. The unpaired electrons of paramagnetic metal ions in close proximity and/or separated by a delocalized electron system (such as the aromatic ring system of daunorubicin), will tend to detect one another and augment their spin relaxation rates through dipolar spin–spin coupling. This increased relaxation rate of the unpaired electron spins in EPR is typically manifested as broadening of the EPR signal, as is observed in Fig. 8. The appearance of the small negative signal at 3550 G suggests that some ferromagnetic coupling between two unpaired electrons of two Cu(II) ions is taking place, leading to the observation of an $S = 1$ EPR signal (i.e. the two electron spin, each +1/2, are oriented in the same direction to give a net spin of 1). These signals have very fast relaxation rates and therefore

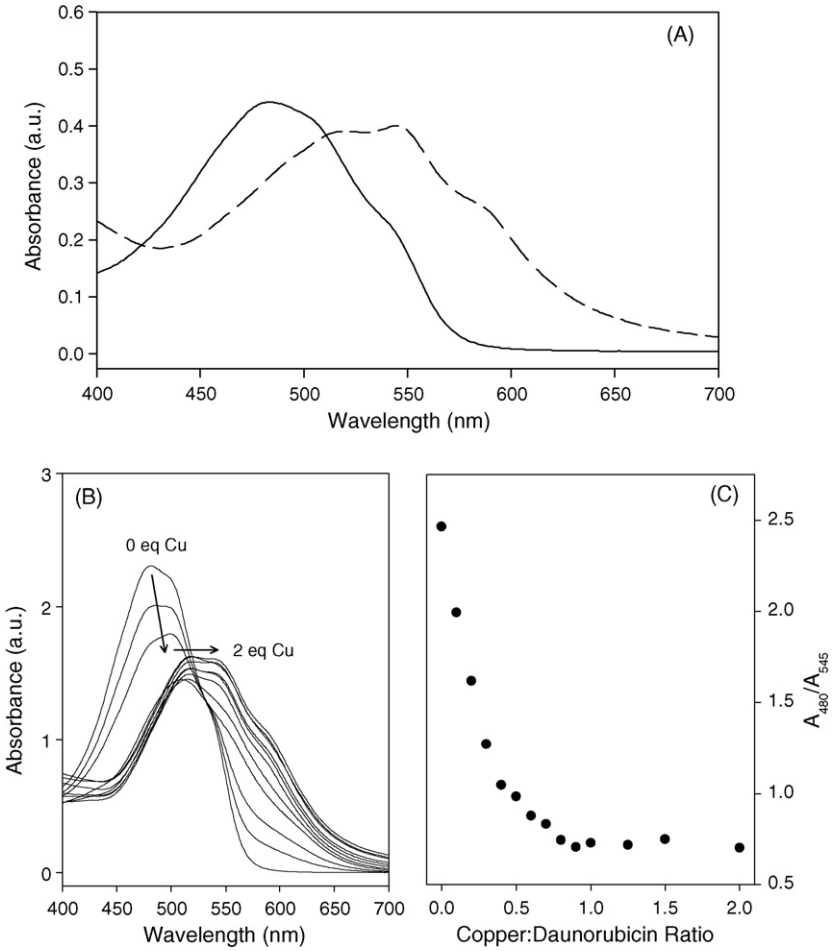

Fig. 7. (A) UV–vis absorbance spectrum of daunorubicin (solid line, 2 mg/mL in SPE buffer at pH 7.4) and CPX-351 (dashed line), measured in a 0.01 cm cuvette at 25 °C. (B) Batch titration of copper gluconate/TEA (0–0.25 mM) into 0.25 mM daunorubicin at pH 7.4 monitored by UV–vis spectroscopy. (C) Absorbance intensity ratio of free daunorubicin (λ = 480 nm) and copper–daunorubicin (λ = 545 nm) as a function of copper:daunorubicin molar ratio.

would be expected to be weak at 77 K. Two hyperfine peaks are observable in the parallel region, at ~2700 G and 2870 G which upon rough simulation yield $g_{||} = 2.271$ and $A_{||} = 175 \times 10^{-4}$ cm^{-1} (Table 2). The features found in the perpendicular region are consistent with either 1:1 or 2:1 copper gluconate/TEA:daunorubicin interactions and determination of the spin Hamiltonian parameters ($g_{||}$ and $A_{||}$) show that this spectrum is distinct from that of CPX-351 ($g_{||} = 2.265$ and $A_{||} = 184 \times 10^{-4}$ cm^{-1}).

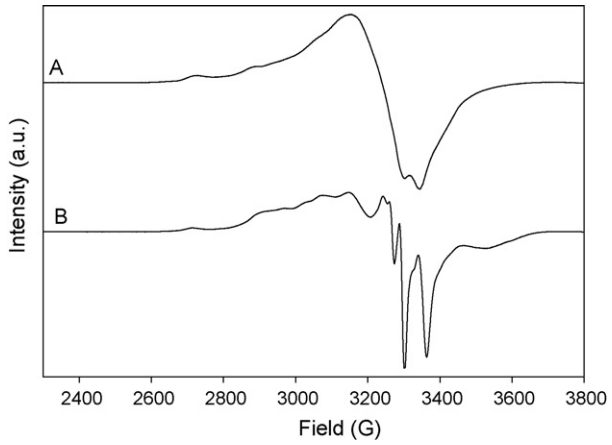

Fig. 8. EPR spectrum of copper gluconate/TEA buffer (20 mM, pH 7.4) in the presence of 1 equiv. (A) and 5 equiv. (B) daunorubicin (T = 77 K, P = 10 mW, modulation amplitude = 10 G, ν = 9.45 GHz).

By contrast, the EPR signal for the 1:5 copper gluconate/TEA:daunorubicin system behaves much more like an isolated $S = 1/2$ system. The perpendicular peak centered at 3300 G has narrowed considerably, and ~4 superhyperfine signals are observable within this region. Observation of 4 superhyperfine peaks is consistent with copper ($I = 3/2$) while observation of 3 lines could be attributable to nitrogen from TEA ($I = 1$). It is not possible to discern from either possibility from this spectrum.

3.4. Role of copper in drug retention

The EPR and UV–vis data shown above clearly demonstrate that copper interacts with daunorubicin. In order to determine what role copper plays in drug retention, we designed variants of CPX-351 with reduced copper contents. Both cytarabine and daunorubicin can be encapsulated into low copper (10 mM) and copper-free liposomes (Fig. 9A). However, for both formulations, we observed a decrease in drug retention compared to CPX-351. Indeed, for the 10 mM copper formulation, approximately 20% of the encapsulated cytarabine leaked out of the liposomes upon subsequent daunorubicin loading (Fig. 9B). This suggests that higher concentrations of copper gluconate/TEA are required to interact with cytarabine and retain the drug inside liposomes. Also, room temperature dialysis of the copper-free formulation resulted in continuous daunorubicin leakage whereas copper containing liposomes did not show any drug release over 2 h. These results indicate

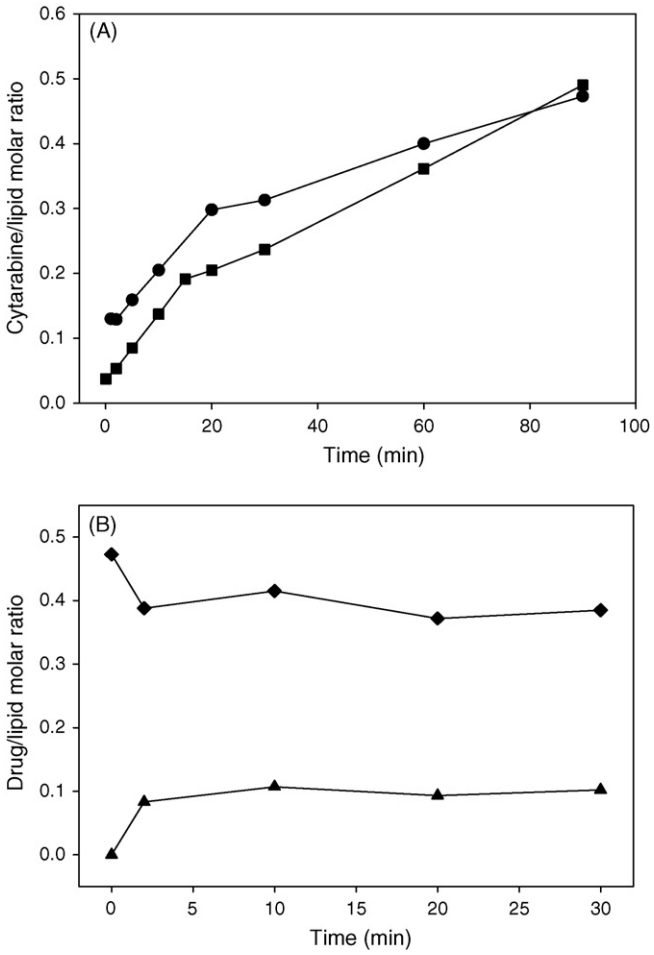

Fig. 9. (A) Cytarabine/lipid molar ratios into liposomes containing: (■) 100 mM sodium gluconate/110 mM TEA, pH 7.4; (●) 10 mM copper gluconate/22 mM TEA, pH 7.4. (B) Liposomal concentrations of cytarabine (♦) and daunorubicin (▲) during daunorubicin encapsulation of the 10 mM Cu formulation (external buffer = SPE).

that copper is indispensable to retain both cytarabine and daunorubicin inside liposomes.

4. Discussion

Due to the macromolecular nature of liposomal intravenous drug delivery systems, the physicochemical properties of liposome-based anticancer drug products can strongly influence pharmacokinetics, toxicity and efficacy performances. The importance of biophysical characterization of liposomal drug product physicochemical properties is reflected in a 2002 draft guidance document from the Center for Drug Evaluation and Research (CDER) at the US FDA entitled "Liposome Drug Products: Chemistry, Manufacturing, and Controls; Human Pharmacokinetics and Bioavailability; and Labeling Documentation". In this document, it is stated that "The physicochemical characterization tests, which are critical to ensuring product quality of each batch of liposome drug product, should be identified". In light of these considerations, we have undertaken extensive scientific investigations to characterize the physicochemical properties of CPX-351.

CPX-351 was designed to deliver synergistic ratios of cytarabine and daunorubicin in vivo for optimal efficacy. In the present study, spectroscopy was used to delineate parameters that play a role in drug retention. CPX-351 contains a transition metal, copper that is known to form strong complexes with daunorubicin in solution (Greenaway and Dabrowiack, 1982). Our UV–vis and EPR data confirmed that such complexes can be formed inside liposomes. Exhaustive characterization of CPX-351 was undertaken to identify the stochiometry of daunorubicin:copper inside liposomes. The lack of spectral changes observed for titration of copper gluconate/TEA into daunorubicin after addition of 1.0 Mequiv. of copper demonstrates that UV–vis spectroscopy cannot be used to differentiate between 2:1 and 1:1 complexes of copper and daunorubicin, respectively. In the case of the 1:1 complex, previous circular dichroism, NMR and UV–vis studies have demonstrated that copper and daunorubicin form a 1:1 repeating oligomer that would place the coordinated copper centers in close proximity to each other (Greenaway and Dabrowiack, 1982). This property would manifest itself in an EPR spectrum in a broadening of the spectral features. A 2:1 complex would likely have a coordination structure similar to the 1:1 oligomer with a copper ion bound to each side of the anthraquinone moiety of daunorubicin. It is unlikely that the 1:1 and 2:1 copper:daunorubicin complexes could be differentiated by EPR. Therefore, the observed EPR spectrum of CPX-351 (Fig. 4), in consideration of the intraliposomal copper and daunorubicin concentrations, is consistent with formation of a 1:1 or 2:1 copper:daunorubicin coordination complex.

Our EPR data also suggest that cytarabine can bind to the copper gluconate/TEA buffer, but only when present in large excess. The cytarabine:copper ratio within CPX-351, however, is approximately 2:1 therefore only a small amount of the total cytarabine present within the formulation could be expected to be interacting with the copper gluconate/TEA buffer at any one time. Besides, a key observation of the NMR spectrum of cytarabine in solution is the interaction stoichiometry; cytarabine is in a 2:1 excess over copper in the top spectrum, yet one resonance is completely absent. This peak is also not observable in a spectrum where cytarabine is at a 7-fold excess of copper (data not shown). It is unlikely for a single copper center to bind 7 cytarabine molecules at one time; rather the cytarabine is likely in a rapid bound/free equilibrium such that during the timescale of the NMR spin transition, all cytarabine molecules are averaged to be copper-bound. This conclusion is supported by the fact that only the proton most closely associated with the metal-binding site of cytarabine is affected, and that EPR suggests only a portion of the cytarabine is bound at any one time.[1] The assignment of the likely binding site for copper on the cytarabine ligand is further supported by reexamination of the EPR spectra in Fig. 5. As cytarabine is added to the solution of copper gluconate/TEA, a slight shift in *g*-factor (i.e. resonant field position) is noted for the parallel hyperfine peaks at 2720 G, 2890 G and 3060 G. The shift is upfield, to smaller *g*-values, consistent with nitrogen coordination to a copper center. Cytarabine possesses two nitrogens in its cytosine moiety that are likely sites for metal ion coordination, and copper coordination to the drug has been reported (Chao and Kearns, 1977). The resonant field values and magnitude of the parallel hyperfine peaks are similar to what is observed in the EPR spectrum of CPX-351. Simulation of the appropriate EPR spectra demonstrated that the spin Hamiltonian values for copper–daunorubicin solutions were dissimilar to those observed for CPX-351. The EPR spectrum of CPX-351 therefore exhibits contributions from both detected drug–excipient interactions, namely copper–cytarabine (parallel region) and copper–daunorubicin (perpendicular region).

Cryo-EM pictures revealed an internal structure inside CPX-351 liposomes. Initially, we hypothesized that the internal ring could be composed of drugs precipitates or lipids. A systematic

[1] This analysis highlights a useful feature of comparison of EPR and NMR spectra; EPR is collected in the frozen state and therefore represents a "snapshot" of the solution chemistry, while the NMR spectrum is collected in a dynamic state, and represents all interactions averaged out over the timescale of the NMR experiment.

Table 3
Surface area calculations for liposomes of known diameter (unloaded, cytarabine-loaded) for determination of amount of total lipid exposed to the external buffer.

Sample	d (nm)	Surface area ($\times 10^6$ Å^2)			% External[a]	% Unquenched[b]
		Outer leaflet	Inner leaflet	Total		
Unloaded	115	4.16	3.46	7.62	54.5	45.5
Cytarabine-loaded	107	3.60	2.96	6.56	54.9	45.1

[a] Calculated as outer/total × 100%.
[b] Calculated as 100% – (% external).

characterization at all steps of the production of CPX-351 was completed and revealed that the internal structure was generated during cytarabine loading and persisted upon daunorubicin loading. Fluorescence quenching of NBD-PE labeled liposomes confirmed that the inner structure was a second lipid bilayer as a greater portion of lipids was quenched in the empty liposomes (unilamellar) compared to the cytarabine-loaded liposomes. This result can be understood by considering the relative amounts of lipid exposed to the external buffer for a unilamellar system and a slightly smaller bilamellar system, generated from the original unilamellar vesicles. Calculation of the surface area of each leaflet of the bilayer(s) can be used to compare the amount of lipid exposed to the external buffer relative to the total amount of lipid required to form one liposome. For this calculation, a bilayer thickness of 5 nm was assumed, such that for a liposome with outer diameter of 115 nm, the inner leaflet would have a diameter of 105 nm. The results of the surface area calculations[2] are presented in Table 3. For the unloaded and cytarabine-loaded samples, the percentage of total lipid found on the outer leaflet (~55%) is nearly identical in both cases; therefore differences in diameter alone between the unloaded and cytarabine-loaded samples cannot explain the difference in quenched lipid. For cytarabine-loaded liposomes, a portion of the total lipid from the unloaded sample is now protected from reductive quenching by dithionite. The difference in total surface area of the two samples (7.62–6.56 = ~1 × 10^6 Å^2) therefore represents the amount of lipid present in the interior liposome space and thus inaccessible to dithionite. Further calculation reveals that this amount of lipid is sufficient to form a 50 nm diameter vesicle within each liposome.

Since the cytarabine-loaded sample was generated from the unloaded liposomes; the total lipid in the system and hence the total lipid per liposome is unchanged. Differences do exist however in the amount of lipid exposed to the external buffer in each system (Table 3, 4.16 versus 3.60 × 10^6 Å^2 for the unloaded and loaded samples, respectively). In the case of the loaded sample, this exposed lipid is now protected in the liposome interior. The percent change in exposed lipid ($\Delta_{exposed}$) between the two systems is calculated as follows:

$$\Delta_{exposed}(\%) = \frac{SA^{outer}_{unloaded} - SA^{outer}_{loaded}}{SA^{outer}_{unloaded}} \times 100$$

In the equation, SA is the surface area of the outer lipid leaflet reported in Table 3 for either the unloaded or cytarabine-loaded sample. This calculation reveals there is a 13.5% reduction in the amount of exposed lipid from the unloaded to the cytarabine-loaded sample. This calculation compares very well to the experimental value determined in Fig. 3C to be (61.6–46.6) = 15%. Therefore, the observed change in liposome diameter upon cytarabine loading can be correlated with the observation of internal structures within the liposomes in the cryo-EM images and decreased accessibility of some of the NBD-labeled lipid headgroups in the cytarabine-loaded sample relative to unloaded liposomes. Taken together, these data indicate that the internal structures within the cryo-EM images are lipid vesicles. CPX-351 is therefore a bilamellar liposome system, a property which is reproducibly induced by the cytarabine loading procedure.

Conditions under which these liposomes are formed were identified and could be generated in a reproducible manner. The measured osmolality of the 50 mM copper, 110 mM TEA buffer with sufficient cytarabine to achieve a 0.5 drug:lipid molar ratio was approximately 6 times greater than the identical buffer solution without cytarabine; a considerable osmotic gradient is therefore generated during the cytarabine loading process. Thus, the second lipid bilayer is believed to result from exposure of the unilamellar liposomes to high temperature and high external osmolarity and was found to be independent of copper gluconate inside liposomes (data not shown). This mechanism of internal lamellae formation is well-supported in the literature (Kas and Sackmann, 1991; Mui et al., 1995). Aqueous lipid bilayers exist in a balance of thermodynamic forces dictated by a drive to minimize water exposure to hydrophobic regions while concomitantly holding the bilayer shape within the constraints imposed by the lipid blend's intrinsic shape (Mui et al., 1995; Cullis et al., 1997). The main descriptor of this balance for any liposome is the surface area-to-volume ratio. For liposomes exposed to a high external osmolality relative to the entrapped buffer, two possible responses can occur; the external solute can be transported inwards through the bilayer to balance the external:internal osmolality, or solvent (water) from the internal buffer can flood out of the entrapped space, thereby increasing the osmolality of the internal buffer and leading to an approximate equilibration of internal and external osmolalities. Since most lipid bilayers are freely permeable to water and much less so to most solutes, typically water egress is the method by which the osmotic challenge is met.

This rapid response leads to an increase in surface area-to-volume ratio, i.e. there is more lipid than required to form a liposome of a given size. This thermodynamic stress leads to invagination of the membrane into the reduced volume space. If the change in internal volume is large enough, the lipid invagination can continue directly into the liposome interior to such a point that the intrinsic curvature limit for the lipid blend is reached and a new vesicle is blebbed into the interior of the original liposome (Kas and Sackmann, 1991; Mui et al., 1995). Temperatures near or beyond the gel to liquid–crystalline phase transition are required so that the lipid membranes are fluid enough to adopt intermediate shapes as the internal invagination proceeds. This process is visually described in Scheme 1.

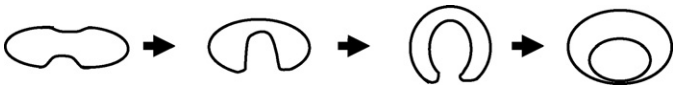

Scheme 1. Schematic diagram of the process of internal lamella formation as a thermodynamic response of the lipid bilayer to decrease the surface area-to-volume ratio of the liposome caused by water egress in response to an external osmotic challenge. Adapted from Kas and Sackmann (1991).

[2] For a sphere, SA = $4\pi r^2$. Values of 62 Å^2, 66 Å^2 and 19 Å^2 for DSPC, DSPG and cholesterol, respectively, were used as the headgroup surface area of the lipid components. A weighted average for the 7:2:1 DSPC:DSPG:Chol system is calculated to 58.5 Å^2 per lipid headgroup.

5. Conclusion

CPX-351 is an injectable formulation of two antineoplastic agents, cytarabine and daunorubicin, where the drugs are encapsulated inside liposomes at a fixed 5:1 molar ratio. The biological activity of this formulation is dependent on the ability to reproducibly control drug loading and retention within the liposomes such that the 5:1 molar ratio of cytarabine:daunorubicin is maintained.

We carried out a variety of biophysical measurements in conjunction with certain chemical analyses of the components in liposomal CPX-351 as well as in solution state to elucidate their physical disposition and interactions with other components. Based on the results for core physicochemical properties (lipid phase transition temperature, liposome morphology, lamellarity, aqueous trapped volume and zeta potential) we can conclude that CPX-351 consists of gel-phase bilamellar liposomes with a strong negative surface potential.

Spectroscopic characterization of CPX-351 detected and quantified extensive drug–buffer excipient interactions. NMR spectroscopy confirmed that, in solution, cytarabine interacted with the copper buffer over the timescale of the experiment. This behaviour was manifested in CPX-351 samples through an increase in the percentage of the total copper that was observed by EPR. UV–vis and EPR data suggested that encapsulation of cytarabine and daunorubicin resulted in formation of a 1:1 or 2:1 daunorubicin:copper species within the liposomes.

We demonstrated that copper was required to retain daunorubicin inside liposomes. Copper was also found to be necessary to prevent cytarabine leakage from liposomes upon daunorubicin loading. These observations clearly show that copper is indispensable in modulating synergistic release of both drugs from the liposomes.

The composition of the inner structure as a lipid bilayer was confirmed through fluorescence labeling and selective reductive quenching of the outer lipid leaflet. The combination of high external buffer osmolality and elevated temperature at or above the phase transition temperature was demonstrated to be responsible for the formation of the bilamellar system during the cytarabine encapsulation step.

Taken together, drug loading and liposome structure of CPX-351 are products of two distinct processes. For cytarabine, passive diffusion of the drug across the liposome membrane appears to be assisted by coordination to the external copper gluconate/TEA buffer system. This process drives the formation of an internal lamella found consistently throughout the formulation, as detected by cryo-EM imaging. In the case of daunorubicin, the drug is rapidly and actively transported across the membrane and subsequently coordinated by the encapsulated copper gluconate/TEA. Copper coordination was found to be critical for retention of both drugs inside liposomes. This demonstrates the role of copper gluconate/TEA in modulating the physicochemical states of both drugs and their coordinated release from the liposomes. It is still unclear what role the second bilayer plays in drug release. More work is underway to elucidate the mechanism of drug release from CPX-351 liposomes.

Acknowledgments

The authors would like to thank Drs. Steve Ansell, Paul Tardi, Sharon Johnstone and Donna Cabral-Lilly for helpful discussions. We are also grateful to Goran Karlsson and Dr. Katarina Edwards at Uppsala University in Sweden for the cryo-EM work and to William Bernt for performing the zeta potential measurements.

References

Abraham, S.A., Edwards, K., Karlsson, G., MacIntosh, S., Mayer, L.D., McKenzie, C., Bally, M.B., 2002. Formation of transition metal-doxorubicin complexes inside liposomes. Biochim. Biophys. Acta 1565, 41–54.

Almgren, M., Edwards, K., Karlsson, G., 2000. Cryo transmission electron microscopy of liposomes and related structures. Colloids Surfaces A: Physicochem. Eng. Aspects 174, 3–21.

Angeletti, C., Nichols, J.W., 1998. Dithionite quenching rate measurement of the inside-outside membrane bilayer distribution of 7-nitrobenz-2-oxz-1,3-diazol-4-yl-labeled phospholipids. Biochemistry 37, 15114–15119.

Batist, G., Miller, W., Mayer, L., Janoff, A., Swenson, C., Louie, A., Chi, K., Chia, S., Gelmon, K., 2007. Ratiometric dosing of irinotecan (IRI) and floxuridine (FLOX) in a phase I trial: a new approach for enhancing the activity of combination chemotherapy. J. Clin. Oncol. 25, 109s.

Batist, G., Gelmon, K.A., Chi, K.N., Miller Jr., W.H., Chia, S.K., Mayer, L.D., Swenson, C.E., Janoff, A.S., Louie, A.C., 2009. Safety, pharmacokinetics, and efficacy of CPX-1 liposome injection in patients with advanced solid tumors. Clin. Cancer Res. 15, 692–700.

Bayne, W.F., Mayer, L.D., Swenson, C.E., 2009. Pharmacokinetics of CPX-351 (cytarabine/daunorubicin HCl) liposome injection in the mouse. J. Pharm. Sci. 98, 2540–2548.

Berger, N.A., Eichhorn, G.L., 1971. Interaction of metal ions with polynucleotides and related compounds XIV: nuclear magnetic resonance studies of the binding of copper(II) to adenine nucleotides. Biochemistry 10, 1847–1857.

Boman, N.L., Masin, D., Mayer, L.D., Cullis, P.R., Bally, M.B., 1994. Liposomal vincristine which exhibits increased drug retention and increased circulation longevity cures mice bearing P388 tumors. Cancer Res. 54, 2830–2833.

Carithers, R.P., Palmer, G., 1981. Characterization of the potentiometric behavior of soluble cytochrome oxidase by magnetic circular dichroism: evidence in support of heme–heme interaction. J. Biol. Chem. 256, 7967–7976.

Cevc, G. (Ed.), 1993. Phospholipids Handbook. Marcel Dekker, New York.

Chao, Y.H., Kearns, D.R., 1977. Magnetic resonance studies of copper(II) interaction with nucleosides and nucleotides. J. Am. Chem. Soc. 99, 6425–6434.

Cullis, P.R., Hope, M.J., Bally, M.B., Madden, T.D., Mayer, L.D., Fenske, D.B., 1997. Influence of pH gradients on the transbilayer transport of drugs, lipids, peptides and metal ions into large unilamellar vesicles. Biochim. Biophys. Acta. 1331, 187–211.

Dicko, A., Frazier, A.A., Liboiron, B.D., Hinderliter, A., Ellena, J.F., Xie, X., Cho, C., Weber, T., Tardi, P.G., Cabral-Lilly, D., Cafiso, D.S., Mayer, L.D., 2008. Intra and inter-molecular interactions dictate the aggregation state of irinotecan co-encapsulated with floxuridine inside liposomes. Pharm. Res. 25, 1702–1713.

Dicko, A., Tardi, P., Xie, X., Mayer, L., 2007. Role of copper gluconate/triethanolamine in irinotecan encapsulation inside the liposomes. Int. J. Pharm. 337, 219–228.

Escandar, G.M., Sala, L.F., 1992. Complexes of Cu(II) with D-aldonic and D-alduronic acids in aqueous solution. Can. J. Chem. 70, 2053–2057.

Greenaway, F.T., Dabrowiack, J.C., 1982. The binding of copper ions to daunomycin and adriamycin. J. Inorg. Biochem. 16, 91–107.

Haran, G., Cohen, L.K., Bar, L.K., Barenholz, Y., 1993. Transmembrane ammonium sulfate gradients in liposomes produce efficient and stable entrapment of amphiphatic weak bases. Biochim. Biophys. Acta 1151, 201–215.

Harasym, T.O., Tardi, P.G., Harasym, N.L., Harvie, P., Johnstone, S., Mayer, L.D., 2007a. Increased preclinical efficacy of irinotecan and floxuridine co-encapsulated inside liposomes is associated with tumor delivery of synergistic drug ratios. Oncol. Res. 16, 361–374.

Harasym, T.O., Tardi, P.G., Johnstone, S.A., Mayer, L.D., Bally, M.B., Janoff, A.S., 2007b. Fixed drug ratio liposomes formulations of combination cancer therapeutics. In: Gregoriadis, G. (Ed.), Liposome Technology, 3rd ed. CRC Press, Boca Raton, FL, pp. 25–48.

Kas, J., Sackmann, E., 1991. Shape transitions and shape stability of giant phospholipid vesicles in pure water induced by area-to-volume changes. Biophys. J. 60, 825–844.

Lasic, D.D., Ceh, B., Stuart, M.C., Guo, L., Frederik, P.M., Barenholz, Y., 1995. Transmembrane gradient driven phase transitions within vesicles: lessons for drug delivery. Biochim. Biophys. Acta 1239, 145–156.

Lasic, D.D., Frederik, P.M., Stuart, M.C., Barenholz, Y., McIntosh, T.J., 1992. Gelation of liposome interior: a novel method for drug encapsulation. FEBS Lett. 312, 255–258.

Li, X., Hirsh, D.J., Cabral-Lilly, D., Zirket, A., Gruner, S.M., Janoff, A.S., Perkins, W.R., 1998. Doxorubicin physical state in solution and inside liposomes loaded via a pH gradient. Biochim. Biophys. Acta 1415, 23–40.

May, P.M., Williams, G.K., Williams, D.R., 1985. Speciation studies of adriamycin, quelamycin and their metal-complexes. Inorg. Chim. Acta 46, 221–228.

Mayer, L.D., Harasym, T.O., Tardi, P.G., Harasym, N.L., Shew, C.R., Johnstone, S.A., Ramsay, E.C., Bally, M.B., Janoff, A.S., 2006. Ratiometric dosing of anticancer drug combinations: controlling drug ratios after systemic administration dictates therapeutic activity in tumor-bearing mice. Mol. Cancer Ther. 5, 1854–1863.

Mayer, L.D., Janoff, A.S., 2007. Optimizing combination chemotherapy by controlling drug ratios. Mol. Interv. 7, 216–223.

McElhaney, R.N., 1982. The use of differential scanning calorimetry and differential thermal analysis in studies of model and biological membranes. Chem. Phys. Lipids 30, 229–259.

McIntyre, J.C., Sleight, R.G., 1991. Fluorescence assay for phospholipid membrane asymmetry. Biochemistry 30, 11819–11827.

Mui, B.L-S., Döbereiner, H.-G., Madden, T.D., Cullis, P.R., 1995. Influence of transbilayer area asymmetry on the morphology of large unilamellar vesicles. Biophys. J. 39, 930–941.
Park, J.W., 2002. Liposome-based drug delivery in breast cancer treatment. Breast Cancer Res. 4, 95–99.
Perkins, W.R., Minchey, S.R., Ahl, P.L., Janoff, A.S., 1993. The determination of liposome captured volume. Chem. Phys. Lipids 64, 197–217.
Pecsok, R.L., Juvet Jr., R.S., 1955. The gluconate complexes. I. Copper gluconate complexes in strongly basic media. J. Am. Chem. Soc. 77, 202–206.
Sengupta, S., Eavarone, D., Capila, I., Zhao, G., Watson, N., Kiziltepe, T., Sasisekharan, R., 2005. Temporal targeting of tumor cells and neavasculature with a nanoscale delivery system. Nature 436, 568–572.
Tardi, P.G., Gallagher, R.C., Johnstone, S., Harasym, N., Webb, M., Bally, M.B., Mayer, L.D., 2007. Coencapsulation of irinotecan and floxuridine into low cholesterol-containing liposomes that coordinate drug release in vivo. Biochim. Biophys. Acta 1768, 678–687.
Tardi, P.G., Dos Santos, N., Harasym, T.O., Johnstone, S.A., Zisman, N., Tsang, A.W., Bermudes, D.G., Mayer, L.D., 2009a. Drug ratio-dependent antitumor activity of irinotecan and cisplatin combinations in vitro and in vivo. Mol. Cancer Ther. 8, 2266–2275.
Tardi, P., Johnstone, S., Harasym, N., Xie, S., Harasym, T., Zisman, N., Harvie, P., Bermudes, D., Mayer, L., 2009b. In vivo maintenance of synergistic cytarabine: daunorubicin ratios greatly enhances therapeutic efficacy. Leuk. Res. 1, 129–139.